# **International Food Research Journal 32(3): 889 - 902 (June 2025)**

Journal homepage: http://www.ifrj.upm.edu.my



# Preparation and characterisation of palm-based tocotrienol-carotenoid emulsion stabilised by hemp protein isolate-ginsenoside emulsifier

Cui, M. Y., Tan, T. B., Fu, M., Cheng, Z. Y., Mat Yusoff, M. and \*Tan, C. P.

Department of Food Technology, Faculty of Food Science and Technology, Universiti Putra Malaysia, 43000 UPM Serdang, Selangor, Malaysia

#### **Article history**

Received: 10 February 2025 Received in revised form: 11 May 2025 Accepted: 8 July 2025

#### **Keywords**

emulsion, plant-based emulsifier, palm-based functional lipids

#### **Abstract**

The present work examined the effects of combining hemp protein isolate (HPI) and ginsenosides (GS) on emulsion stability. Emulsifiers at various HPI-to-GS ratios (1:0, 0.75:0.25, 0.5:0.5, 0.25:0.75, and 0:1) were evaluated. FT-IR spectroscopy revealed that GS formed hydrogen bonds with HPI, and modified its secondary structure, reducing  $\beta$ -sheet content and exposing hydrophobic regions. The mixed emulsifier showed significantly improved emulsifying activity, stability, and antioxidant capacity compared to pure HPI (p < 0.05). The emulsion prepared using a mixed emulsifier at 0.5:0.5 HPI to GS ratio exhibited smaller particle sizes (253.6  $\pm$  4.3 nm), higher zeta potentials (-42.7  $\pm$  1.0 mV), improved encapsulation efficiency (98.89%), and a more uniform particle size distribution, all of which contributed to stability enhancement. Additionally, the emulsions prepared with mixed emulsifier showed good storage stability (14 d) and thermal stability, but demonstrated poor resistant to ionic strength and freeze-thaw cycles. Overall, HPI-GS complexes showed promise as effective emulsifiers for producing stable emulsions.

<u>DOI</u>

https://doi.org/10.47836/ifrj.32.3.22

© All Rights Reserved

#### Introduction

Carotenoids in palm oil are primarily  $\alpha$ - and  $\beta$ carotenes, which contain long chains of conjugated double bonds that contribute to their provitamin A activity and antioxidant potential, thereby helping to prevent vitamin A deficiency (Mba et al., 2015). Tocotrienols, which are lipid-soluble antioxidants also known as vitamin E, are also abundant in palm oil. The three main tocotrienols found in palm oil are γ-tocotrienol, α-tocotrienol, and δ-tocotrienol (Sundram et al., 2003). Studies have shown that tocotrienols possess various health benefits, including anti-cancer and cholesterol-lowering effects (Colombo, 2010). However, both carotenoids and tocotrienols exhibit low resistance to environmental stressors, such as light exposure and oxidation. Additionally, their direct ingestion results in poor bioavailability due to low solubility in the gastrointestinal fluids and instability in acidic conditions (Fu et al., 2014; Shishir et al., 2018). To overcome these limitations, the use of emulsionbased delivery systems has been extensively researched and demonstrated to be effective (Goh *et al.*, 2015; Chen *et al.*, 2017; Tan *et al.*, 2021).

Proteins, as amphiphilic biomacromolecules, can stabilise emulsions by adsorbing at the oil-water interface, and surrounding dispersed oil and air droplets. There is growing interest in the use of plantbased proteins as alternatives to animal-derived emulsifiers due to their favourable digestibility, environmentally sustainability, and health benefits (Silva et al., 2019; Kim et al., 2020; Xiao et al., 2023). However, plant proteins often have limited solubility and poor emulsifying properties, making it necessary to develop effective and cost-effective strategies to enhance their functionality. This can be achieved by modifying the protein structure to expose hydrophobic amino acid residues that are typically buried within the protein core. Physicochemical and enzymatic modification methods such as heat treatment, ultrasound processing, and oxidation have been employed to enhance the emulsifying capacity of plant proteins (Chen et al., 2023; Lima et al., 2023;

Rajasekaran et al., 2023; Shi et al., 2023; Zhang et al., 2023; Han et al., 2024; Igartúa et al., 2024). In addition, conjugation with polysaccharides, polyphenols, and saponins under controlled pH and mixing conditions has proven to be an effective and economical method for improving emulsifying performance (Evans et al., 2013; Li et al., 2021; Liu et al., 2023a; 2023b; Sun et al., 2023).

The global cultivation of hemp seed has increased significantly, and hemp protein isolate (HPI) is gaining attention due to its balance amino acid composition, good digestibility, and functional properties (Shen et al., 2021). Studies have shown that the conjugation of HPI with polysaccharides or polyphenols can improve its emulsifying capacity, enabling the formation of stable emulsion systems (Liu et al., 2023a; 2023b; Gholivand et al., 2024). However, the potential of combining HPI with saponins has not been thoroughly explored. While most studies on saponin-based emulsifiers have focused on Quillaja and tea saponins, ginsenosides (GS), a class of triterpenoid saponin extracted from remain relatively underutilised. ginseng, Ginsenosides are bioactive compounds known for their multifunctional properties, including anticancer, anti-inflammatory, anti-fatigue, and antiaging effects (Li et al., 2023a; Tian et al., 2023), making them promising functional ingredients for food applications.

Recent studies have demonstrated combining plant-based proteins with saponins can enhance emulsifying properties, and improve emulsion stability through synergistic interactions (Xu et al., 2021; Yan et al., 2022; Sun et al., 2023). Therefore, the present work was focused on the combination of HPI and GS to develop a stable palmbased functional lipid emulsion. The prepared oil phase enriched with palm-based tocotrienol and carotenoid, and the emulsions stabilised by an emulsifier formed through simple mixing of two natural ingredients (HPI and GS) contained various nutritional and functional components, and would significantly enhance the nutritional and functional value of the emulsions.

#### Materials and methods

Materials

Hemp protein isolate (90% protein) and ginsenosides (80% saponin) were purchased from Realin Biotechnology Co., Ltd. EvNol (50%

tocotrienol), EVTene (20% carotenoid), and mediumchain triacylglycerol (MCT) oil were purchased from ExcelVite Sdn. Bhd. Analytical-grade chemicals were used in the present work.

# Preparation of HPI-GS complex

HPI and GS were dissolved in deionised water to prepare 1% (w/v) solution based on the active ingredients, and stored at 4°C overnight. The HPI solution was centrifuged at 8,000 rpm for 20 min, and the supernatant was collected for subsequent analyses. Mixed HPI and GS solutions in the ratios of 1:0, 0.75:0.25, 0.5:0.5, 0.25:0.75, and 0:1, which were labelled as A, B, C, D, and E, were stirred with a rotor for 2 h.

Fourier transforms infrared (FT-IR) measurement

The FT-IR spectra of different mass ratios (1:0, 0.75:0.25, 0.5:0.5, 0.25:0.75) of HPI and GS freezedried powder at neutral pH was measured at a range of 4000 - 400 cm<sup>-1</sup> using a FT-IR Spectrometer (Bruker, Invenio-R, Billerica, USA).

# Free sulfhydryl ( $SH_F$ ) content analysis

The protein sample (1 mL, 2.5 mg/mL) was mixed with 4 mL of buffer A (0.1 M pH 8.0 Trisglycine solution, 1 M urea, 0.01 M EDTA) and 125  $\mu$ L of buffer B (0.1 M pH 8.0 Tris-glycine, 0.01 M DTNB), incubated at 25°C for 1 h in the dark, and centrifuged at 10,000 g for 15 min, and the absorbance of the supernatant was measured at 412 nm (Feng *et al.*, 2022). The SH<sub>F</sub> was calculated using Eq. 1:

SH<sub>F</sub> (
$$\mu$$
mol/g) = 73.53 ×  $A_{412}$  ×  $\frac{D}{C}$  (Eq. 1)

where, D = dilution factor, and C = concentration of sample.

#### Free amino groups

Briefly, 40 mg of OPA was dissolved in 1 mL of ethanol, and sequentially added to 2.5 mL of 20% (m/v) SDS solution, 25 mL of 0.1 M sodium tetraborate solution, and 0.1 mLof ßmercaptoethanol, then adjusted to a final volume of 50 mL. Next, 0.2 mL of the sample solution (with protein content diluted to 2 mg/mL) was added with 4 mL of OPA reagent, and incubated at 35°C for 2 min. The absorbance was then measured at 340 nm (Liu et al., 2021). Distilled water was used as a blank control.

Antioxidant activity of HPI-GS complexes ABTS method

Briefly, 7 mmol/L ABTS was prepared and mixed with 2.45 mmol/L potassium persulphate in equal amounts. 12 - 16 h of reaction was needed to compete the radical generation in the dark at room temperature. It was then diluted with ethanol so that its absorbance was adjusted to  $0.70 \pm 0.02$  at 734 nm. Next, 4 mL of ABTS solution was mixed with 70  $\mu$ L of the sample (10 mg/mL), and incubated for 6 min. Then, its absorbance was measured at 734 nm. The ABTS radical scavenging activity (%) was calculated using Eq. 2:

ABTS radical scavenging activity (%) = 
$$\frac{A_b - A_s}{A_b} \times 100$$
 (Eq. 2)

where,  $A_b$  = absorbance of the blank, and  $A_s$  absorbance of the sample.

Ferric-reducing antioxidant power (FRAP) assay

Briefly, 0.031 g of 2,4,6-tris(2-pyridyl)-striazine (TPTZ) was dissolved in 10 mL of 40 mM HCl to prepare TPTZ solution (10 mM). Next, 0.054 g of FeCl<sub>3</sub>·6H<sub>2</sub>O was dissolved in 10 mL of deionised water to prepare ferric chloride solution (20 mM). Then, acetate buffer (300 mM, pH 3.6) was prepared by dissolving 3.1 g of sodium acetate trihydrate in 16 mL of acetic acid, made up to 1 L using deionised water, and its pH was adjusted to 3.6. Finally, the FRAP reagent was prepared by mixing 100 mL of acetate buffer, 10 mL of TPTZ solution, and 10 mL of ferric chloride solution. Afterward, 3 mL of FRAP reagent was added with 100 µL of the sample, and incubated at 37°C for 4 min before measuring the absorbance at 593 nm. Deionised water mixed with 3 mL of FRAP reagent served as blank. Using the constructed standard curve (y = 0.7533x - 0.0259,  $R^2$ = 0.9992), the FRAP values of the samples were then calculated.

Emulsifying activity index (EAI) and emulsion stability index (ESI)

MCT (10%, v/v) were added into mixed solutions. High-shear homogeniser (Silverson L4R, Buckinghamshire, UK) was used to prepare coarse emulsions by operating at 8,000 rpm for 2 min. Next, 20 µL of the emulsions from the bottom layer were extracted immediately, mixed with 5 mL of 0.1% sodium dodecyl sulphate (SDS) solution, and

incubated for 10 min. Absorbance of mixture was measured at 500 nm, and deionised water was used as a blank. The EAI and ESI were calculated using Eqs. 3 and 4:

EAI 
$$(m^2/g) = 2 \times 2.303 \times \frac{N \times A_0}{c \times \phi \times 10000}$$
 (Eq. 3)

$$ESI (min) = \frac{A_0 \times \Delta t}{A_0 - A_{10}}$$
 (Eq. 4)

where, N = dilution factor,  $\phi$  = volume fraction of the oil phase in the emulsion, c = concentration of the emulsifier solution,  $\Delta t$  = time interval between two measurements, and  $A_0$  and  $A_{10}$  = absorbances measured at 0 min and 10 min, respectively.

#### Preparation of oil phase and emulsion

For oil phase, 0.4 g of carotenoid and 3.6 g of tocotrienol were added to 96 g of MCT oil, and stirred for 50 min at 55°C and 200 rpm. HPI and GS were each dissolved in deionised water to form 1% (w/v) solution based on their active compounds, and the solutions were stored at 4°C overnight. The HPI solution was then centrifuged at 8,000 rpm for 20 min, and the supernatant was collected for further use. HPI and GS were mixed in the desired ratios, and stirred with a rotor at neutral pH for 2 h. The compositions of emulsifier, oil phase, and water phase are detailed in Table 1.

A high-shear homogeniser (Silverson L4R, Buckinghamshire, UK) was used to prepare 200 mL of coarse emulsions by operating at 6,000 rpm for 5 min. Subsequently, the coarse emulsions were subjected to high-pressure homogenisation using a high-pressure homogeniser (Panda 2 K, Niro Soavi, Deutschland, Lubeck, Germany) at 500 bar for three cycles.

**Table 1.** Proportions of emulsion composition.

	W	Oil		
Emulsion	Water (%, m/v)	HPI (%, m/v)	GS (%, m/v)	phase (%, v/v)
A	89.1	0.9	0	10
В	89.1	0.675	0.225	10
C	89.1	0.45	0.45	10
D	89.1	0.225	0.675	10
Е	89.1	0	0.9	10

#### Encapsulation efficiency

To assess the encapsulation efficiency of emulsions with varying emulsifier ratios, 2 mL of emulsion was mixed with 5 mL of hexane. After vortexing for 1 min, the mixture was centrifuged at 4,000 g for 5 min. The organic phase of the supernatant was then separated and placed in a fume hood to allow the hexane to evaporate completely. The mass of the sample container before the addition of the organic phase and after the volatilisation of the organic phase were denoted as m<sub>1</sub> and m<sub>2</sub>, respectively. Next, Eq. 5 was used to calculate the encapsulation efficiency:

$$EE (\%) = (1 - \frac{m_2 - m_1}{0.182}) \times 100\%$$
 (Eq. 5)

where, 0.182 = mass of oil phase in 2 mL of emulsion.

Particle size, polydispersity index (PDI), zeta potential, and particle size distribution (PSD)

The emulsions was diluted with deionised water by a factor of 100 to minimise multiple scattering issues. Zetasizer Nano ZS (Worcestershire, U.K.) instrument was used to measure the particle size, zeta potential, PDI, and PSD. The refractive index ratio was set at 1.460.

# Stability of emulsion

Storage stability

After completion of the emulsion preparation, it was stored at 4°C for 14 d. The particle size distribution of the emulsion was measured at 1, 7, and 14 d.

### Temperature stability

After the emulsion was subjected to a water bath heating at slightly modified conditions approximating those of pasteurisation in terms of temperature and duration (63°C/30 min, 90°C/10 min) (Liu *et al.*, 2023a), it was immediately cooled to room temperature under running tap water. Then, the particle size distribution was measured after incubation at room temperature for 12 h.

#### Ionic strength stability

Different quantities of sodium chloride were added to the emulsion to achieve final concentrations of 50, 100, 250, and 500 mM. They were then observed after incubation at room temperature for 12 h.

# Freeze-thaw stability

The emulsion was stored at -20°C for 24 h, thawed at room temperature for 24 h, and observed.

## Statical analysis

All experiments were conducted in triplicate, and the data were analysed using SPSS, and expressed as mean  $\pm$  standard deviation. One-way ANOVA were performed to evaluate the significance of differences, with a 95% confidence interval (p < 0.05). Following a significant ANOVA result, Fisher's Least Significant Difference (LSD) test was employed for pairwise comparisons to identify specific group differences.

#### Results and discussion

# FT-IR spectroscopy

FT-IR was utilised to analyse the interactions between HPI and GS. According to reports, amide I (1600 - 1700 cm<sup>-1</sup>), which represents the stretching vibration of the amide C=O bond, and amide II (1600 - 1500 cm<sup>-1</sup>), which represents the bending vibration of the N-H bond, are associated with the formation of hydrogen bonds (Gallagher, 2009). From Figure 1, it can be observed that with the increase in the proportion of GS in the mixture, the absorption peak of the amide band shifts from 1640 cm<sup>-1</sup> in A to 1642 cm<sup>-1</sup> in B and C. This shift can be interpreted as the formation of hydrogen bonds induced by the addition

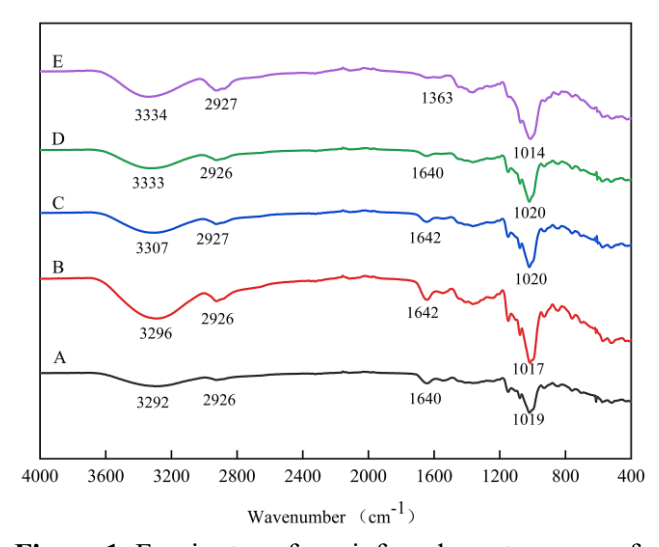


**Figure 1.** Fourier transform infrared spectroscopy of HPI-GS mixture. A, B, C, D, and E represent five different emulsifiers composed of mixtures of HPI and GS at ratios of 1:0, 0.75:0.25, 0.5:0.5, 0.25:0.75, and 0:1, respectively.

of GS, compared to pure HPI. The absorption peaks of 3200 - 3600 cm<sup>-1</sup> and 2800 - 3000 cm<sup>-1</sup> represented O-H and C-H stretching vibration, respectively, and the shifts of these absorption also indicated the formation of hydrogen bonds (Sun et al., 2023). Hydrogen bond is considered, alongside hydrophobic interactions, the most important force in the interaction between proteins and saponins. According to relevant studies, the sugar chains in saponins can form hydrogen bonds with the sugar residues of proteins, resulting in the formation of an adsorbed layer with high surface elasticity (Li et al., 2023b). Besides, the absorption peak of 1000 - 1200 cm<sup>-1</sup> is typically associated with the structure of glycosyl groups, which is caused by C-O and C-O-C vibrations (Zhang et al., 2024). The shift in the absorption peak at this region may be due to interactions between the glycosidic portion of the saponin and protein molecules which is regarded as the result of the combined effects of electrostatic forces and hydrophobicity (Jourdain et al., 2009), leading to changes in the C-O or C-O-C vibrational modes.

#### Secondary structure of HPI

The secondary structure of the protein was obtained from FT-IR data. After converting the transmittance data obtained from FT-IR absorbance, baseline correction and deconvolution were performed, followed by second derivative analysis. As shown in Table 2, consistent with the findings reported by Xu et al. (2022), the primary secondary conformation of HPI was β-sheet. Compared to A, the proportion of  $\beta$ -sheet in B, C, and D significantly decreased, while the proportions of the other three structures increased to varying degrees. This can be understood as a transformation of  $\beta$ -sheet into other three structures. According to the report by Wang et al. (2014), the decrease in β-sheet is associated with the exposure of hydrophobic sites on the protein. Therefore, with the addition of GS, the conformation of the system improved, and exposed more hydrophobic residues and free sulfhydryl which is beneficial for enhancing its emulsifying properties (Li et al., 2023b). It is noteworthy that ginsenosides, as triterpenoid saponins, can modify the secondary structure proteins through hydrophobic interactions, reducing β-sheet content, and exposing more hydrophobic groups, without disrupting the primary structure of the proteins (Kaspchak et al., 2020). The subsequent EAI and ESI measurement also confirmed this improvement.

**Table 2.** Secondary structure of HPI.

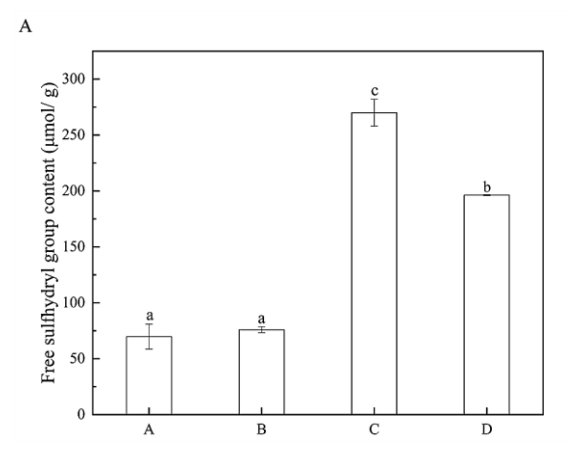
	α-helix	β-sheet	β-turn	Random
				coil
A	16.2	50.4	11.3	22.1
В	19.7	39.1	14.8	26.4
C	18.4	42.4	13.2	26.0
D	18.5	42.2	13.1	26.2

Free sulfhydryl content analysis

The increase in free sulfhydryl content is typically associated with the cleavage of disulphide bonds, which leads to partial unfolding of the protein, and the exposure of more hydrophobic sites and groups (Feng et al., 2022). As shown in Figure 2, the addition of a small amount of GS (B) did not result in a significant increase in free sulfhydryl content compared to A. However, with the increasing proportion of GS (C and D), there was a noticeable increase in free sulfhydryl content, indicating that the addition of GS caused significant structural changes in HPI. This may due to the strengthening of hydrophobic interactions when proteins and saponins were mixed in a specific ratio (C), resulting in the disruption of intermolecular disulphide bonds, and the formation of free sulfhydryl (Xue et al., 2020). The absence of a significant change in free thiol content in sample B can be attributed to the relatively low volume fraction of added saponins (25%). At this concentration, the interfacial properties were primarily dominated by the proteins, and the hydrophobic interactions between saponins and proteins were minimal. Consequently, the free thiol content in sample B showed only a slight, statistical non-significant increase (p > 0.05). According to report of Ma et al. (2020), the exposure of more hydrophobic regions enabled the system to adsorb more effectively at the oil-water interface, thereby forming a stable emulsion.

# Free amino group analysis

Unlike the decrease in the number of free amino groups in protein caused by binding with polysaccharides (Wu et al., 2023), it can be observed from Figure 2 that as the proportion of saponin increased, the number of free amino groups in protein also exhibited an upward trend. This indicated that the interactions occurring between HPI and GS involved either no covalent bonding or only minimal covalent interactions that would typically lead to a decrease in the number of free amino groups. The increase in free



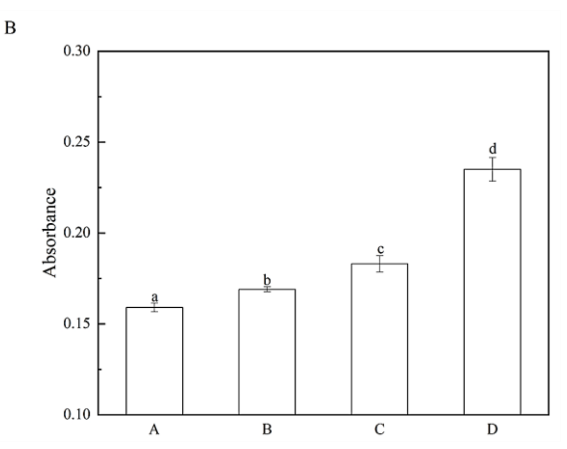


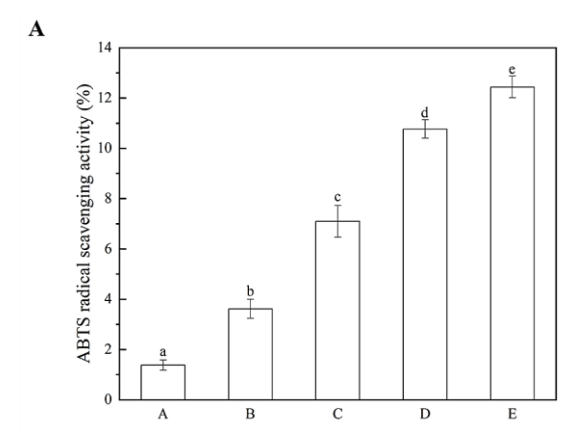
**Figure 2.** Free sulfhydryl content (**A**) and free amino groups analysis (**B**) of HPI. A, B, C, and D represent four different emulsifiers composed of mixtures of HPI and GS at ratios of 1:0, 0.75:0.25, 0.5:0.5, and 0.25:0.75, respectively. Different lowercase letters on error bars indicate significant difference among emulsifier groups by Fisher's LSD test (p < 0.05).

amino groups in protein may be attributed to the fact that the addition of saponin induced a partial unfolding of the protein structure, and reduced the surface tension of the solution, thereby exposing more amino groups within the protein.

#### Antioxidant activity

The ABTS and FRAP methods were used to characterise the antioxidant properties of HPI-GS complexes. Notably, the DPPH which was commonly used in antioxidant studies was not employed because the complexes interfered with the results, causing absorbance to exceed initial values. As shown in Figure 3, both methods for determining antioxidant capacity indicated a gradual increase in antioxidant activity with increasing proportion of saponin. There are two explanations for this phenomenon. Firstly, as

the saponin ratio increased, the free sulfhydryl content in C and D also increased. According to Karabulut *et al.* (2022), there is a positive correlation between the increase in free sulfhydryl content of hemp protein and its antioxidant activity. Therefore, the introduction of saponin altered the protein conformation, enhancing its antioxidant properties. The second reason is the inherent strong antioxidant capacity of ginsenosides, primarily due to the glucose-arabinose group at C-20 and the disaccharide group at C-3 (Chae et al., 2010). These two factors together enhanced the antioxidant capacity of HPI-GS, and higher antioxidant properties of the complexes are significant for stabilising emulsions and inhibiting lipid oxidation (McClements and Decker, 2018).



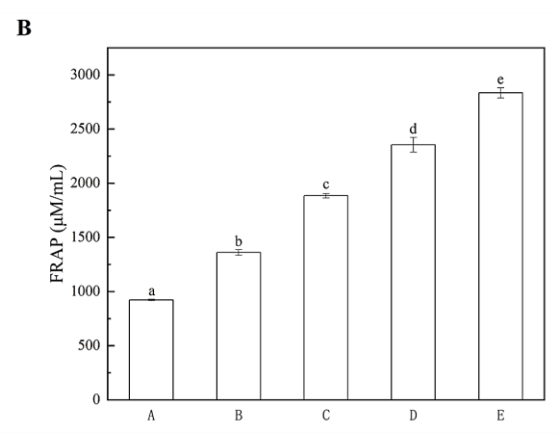


**Figure 3.** Antioxidant activity of HPI-GS mixture. ABTS radical scavenging activity **(A)**, and FRAP **(B)**. A, B, C, D, and E represent five different emulsifiers composed of mixtures of HPI and GS at ratios of 1:0, 0.75:0.25, 0.5:0.5, 0.25:0.75, and 0:1, respectively. Different lowercase letters on error bars indicate significant difference among emulsifier groups by Fisher's LSD test (p < 0.05).

## Emulsifying properties

Emulsifying activity and emulsifying stability are crucial indicators for evaluating the performance of emulsifiers. As shown in Figure 4, with the addition of GS, the emulsifying activity and stability of the mixed emulsifier system composed of HPI and GS (B, C, and D) were significantly improved compared to pure HPI (A), and both values of B showed higher level among them. It was noteworthy that when GS was used alone as an emulsifier (E), although its emulsifying activity was comparable to that of the mixed emulsifiers, its emulsifying stability was very low, even lower than that of A, which indicated poor emulsification stability. Therefore, it can be concluded that mixing protein and saponin in a certain ratio could lead to interactions between them, resulting in structural changes in the protein and saponins which enhanced the emulsifying properties of the mixture.

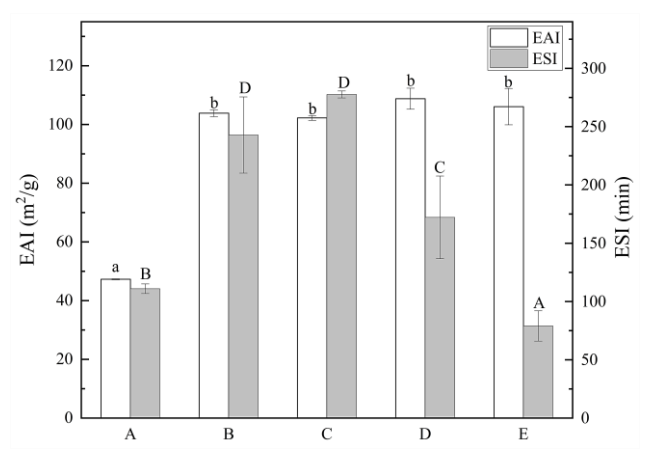


**Figure 4.** Emulsification properties of HPI-GS mixture. A, B, C, D, and E represent emulsion samples prepared with five different emulsifiers composed of mixtures of HPI and GS at ratios of 1:0, 0.75:0.25, 0.5:0.5, 0.25:0.75, and 0:1, respectively.

#### Characterisation of emulsion

The particle size, zeta potential, and PDI of emulsions are primary indicators for evaluating emulsion quality. As indicated in Table 3, the particle sizes of the prepared emulsions were all less than 300 nm. The emulsions prepared using HPI and GS alone (A and E) as emulsifiers exhibited larger particle sizes compared to those prepared with the three different mixed emulsifiers. This may be attributed to the introduction of GS, which altered the interfacial composition of the droplets, leading to competition between the two components for interfacial area and resulting in emulsions with smaller particle sizes (Wilde et al., 2004). Smaller particle sizers signify emulsion quality, and enhance bioavailability of active substances, such as βcarotene (Salvia-Trujillo et al., 2013). The zeta potential absolute value greater than 30 mV is considered advantageous for maintaining emulsion stability, as higher surface potential enhances repulsive interactions between particles, thereby stabilising the emulsion (Lowry et al., 2016). Based on Table 3, the absolute values of zeta potential for all five emulsions exceed 30 mV, with emulsion C exhibiting the highest zeta potential at  $-42.7 \pm 1.0$ mV. The PDI value reflects the width of particle distribution within the emulsion, a PDI value less than 0.3 indicates uniform particle distribution (Sharif et al., 2017). As shown in Table 3, the PDI values of the first three emulsions (A, B, and C) were below 0.3, suggesting uniform distribution. In emulsions D and E exhibited slightly wider distribution compared to the first three. Figure 5 also shows that the particle sizes of all five emulsions presented a unimodal distribution, indicating uniform distribution, which was beneficial for emulsion stability. In terms of encapsulation efficiency,

**Table 3.** Characterisation of palm-based tocotrienol-carotenoid emulsions.

	Particle size (nm)	Zeta potential (mV)	PDI	EE (%)
A	$266.6 \pm 5.2^{\text{b}}$	$-35.1 \pm 3.9^{\text{b}}$	$0.252 \pm 0.019^{b}$	$93.03 \pm 0.76^{a}$
В	$247.6 \pm 1.0^{\circ}$	$-35.3 \pm 0.1^{\text{b}}$	$0.232 \pm 0.008^{b}$	$97.78 \pm 1.56^{b}$
$\mathbf{C}$	$253.6 \pm 4.3^{\circ}$	$-42.7 \pm 1.0^{\rm a}$	$0.246 \pm 0.005^{b}$	$98.89 \pm 0.00^{c}$
D	$265.3\pm0.3^{\text{b}}$	$-32.3 \pm 0.7^{b}$	$0.302 \pm 0.038^{ab}$	$98.90\pm0.00^{c}$
E	$286.3 \pm 4.2^{\mathrm{a}}$	$\text{-}39.9 \pm 1.0^{\text{ab}}$	$0.360 \pm 0.014^{\rm a}$	$99.45\pm0.78^{c}$

Values are mean  $\pm$  standard deviation of five replicates (n = 5). Means in similar column with different lowercase superscripts are significantly different (p < 0.05). PDI: polydispersity index; and EE: encapsulation efficiency.

emulsion A exhibited the lowest efficiency at 93.03%. As the proportion of saponin increased, the encapsulation efficiency of the emulsions gradually improved. Emulsion B's efficiency increased to 97.78%, while emulsions C, D, and E showed no significant differences, each achieving nearly 100% efficiency. This indicated that HPI-GS mixture could be an effective emulsifier for encapsulation, and helped to improve the bioavailability of functional lipids.

In summary, emulsion C demonstrated the lowest particle sizes and PDI values, along with zeta potentials conducive to maintaining emulsion stability and high in encapsulation efficiency, indicating that the specific ratios of HPI-GS mixed emulsifiers performed effectively.

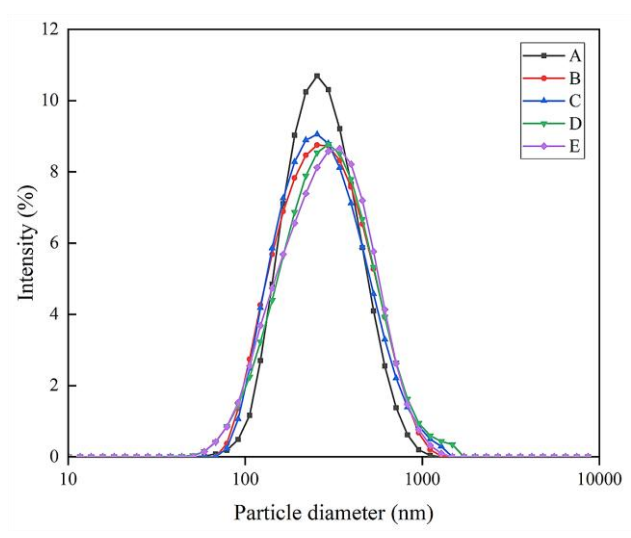


**Figure 5.** Particle size distribution of emulsions prepared by different ratios of HPI-GS mixture. A, B, C, D, and E represent emulsion samples prepared with five different emulsifiers composed of mixtures of HPI and GS at ratios of 1:0, 0.75:0.25, 0.5:0.5, 0.25:0.75, and 0:1, respectively.

#### Stability of emulsion

The stability of the emulsions was analysed considering four factors: storage, temperature, ionic strength, and freeze-thaw cycles.

#### Storage stability

From Figures 6 and 7, it can be observed that both particle size and zeta potential exhibit varying degrees of increase during the storage period of the emulsions. In terms of particle size changes, although all particle sizes had increased, they all remained below 300 nm. Notably, the particle size of emulsion

B, despite its increased, remained the smallest among the five emulsions. From the perspective of zeta potential, during the entire storage period, the zeta potential of all emulsions, expect for emulsion C, showed varying degrees of increase. This increase could be related to the oxidation of the emulsifier, and

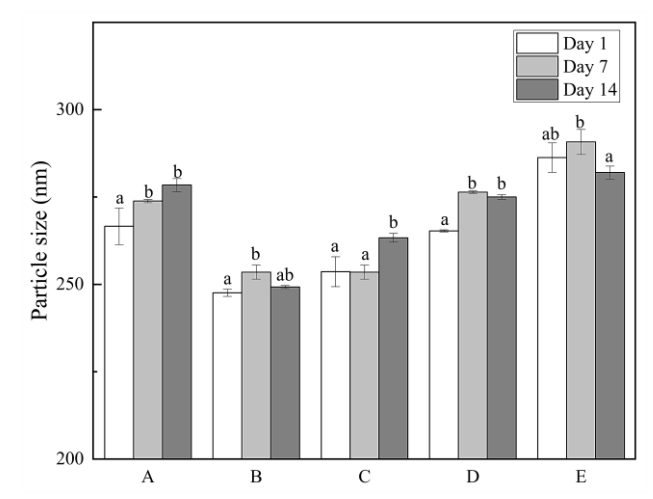


**Figure 6.** Effect of storage duration on particle size of emulsion. A, B, C, D, and E represent emulsion samples prepared with five different emulsifiers which represent the mixtures of HPI and GS at ratios of 1:0, 0.75:0.25, 0.5:0.5, 0.25:0.75, and 0:1, respectively. Different lowercase letters on error bars indicate significant difference among emulsifier groups by Fisher's LSD test (p < 0.05).

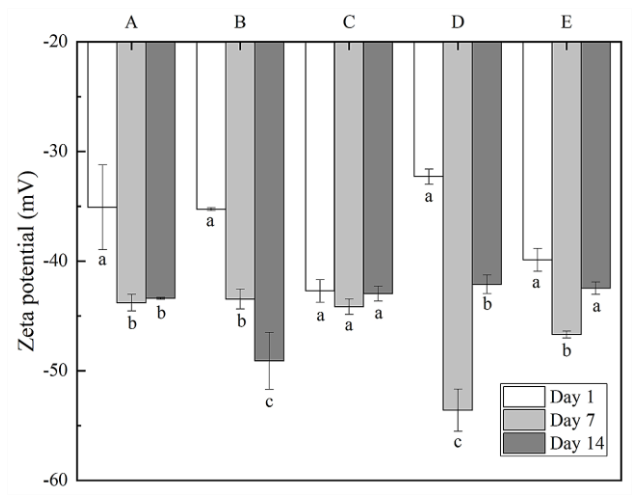


**Figure 7.** Effect of storage duration on zeta potential of emulsion. A, B, C, D, and E represent emulsion samples prepared with five different emulsifiers composed of mixtures of HPI and GS at ratios of 1:0, 0.75:0.25, 0.5:0.5, 0.25:0.75, and 0:1, respectively. Different lowercase letters on error bars indicate significant difference among emulsifier groups by Fisher's LSD test (p < 0.05).

the enhanced interaction of HPI-GS (Li *et al.*, 2022). A surface potential with an absolute value higher than 30 mV also ensured the stability of the emulsion during storage. Figure 8 shows that, except for emulsion E, the peak shape of the particle size

distribution of the other emulsions did not show significant changes, suggesting good stability during storage. Observations of visual images revealed that none of the five emulsions exhibited oil-water separation during the storage period.

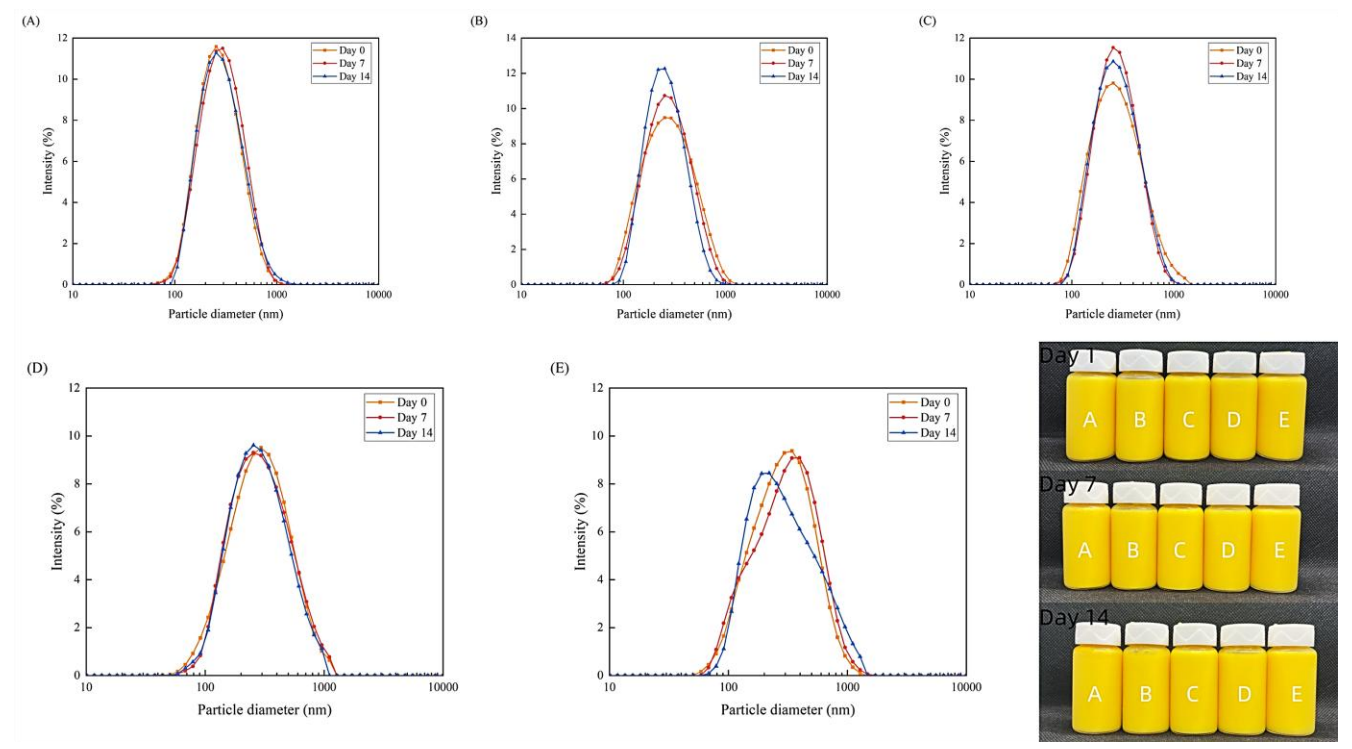


**Figure 8.** Effect of storage duration on particle size distribution and the visual images. Figures A, B, C, D, and E correspond to the five different emulsion samples which prepared with five different emulsifiers composed of mixtures of HPI and GS at ratios of 1:0, 0.75:0.25, 0.5:0.5, 0.25:0.75, and 0:1, respectively.

# Temperature stability

From Figure 9, it can be seen that, except for emulsion A, which exhibited a significant increase in particle size after being heated at 90°C for 10 min, the other emulsions did not show a significant increase in particle size after heating. This indicated that emulsions B, C, D, and E had good resistance to heat treatment. Analysis of the impact of heat treatment on zeta potential from Figure 10 revealed that the absolute value of the zeta potential for emulsion D dropped below 30 mV after being heated at 90°C, which was unfavourable for maintaining emulsion stability. Emulsions B, C, and E exhibited similar changes after being heated at 63 and 90°C. The zeta potential decreased after heating at 63°C for 30 min but increased after heating at 90°C for 10 min, generally remaining above 30 mV. Figure 11 shows that, except for emulsion E, which exhibited a change in peak shape, the other four emulsions did not undergo significant changes. Observations of the images revealed that, after being stored at room

temperature for 12 h following heat treatment, emulsion A exhibited a thin oil layer on the surface at both heating temperatures, indicating poor thermal stability when HPI was used as the emulsifier.

#### *Ionic strength and freeze-thaw stability*

As shown in Figure 12, emulsion A exhibited the best performance in terms of ionic strength stability, and as the proportion of saponin in the emulsifier increased, the degree of oil-water separation gradually became more pronounced. Particularly for emulsion E, even at the minimum addition level of 50 mM, complete oil-water separation occurred, indicating that saponin had very poor resistance to salt. This may be due to the electrostatic shielding effect induced by the addition of sodium chloride (Chen *et al.*, 2024). Proteins have a certain resistance to salt solutions, but saponin have poor resistance, leading to oil droplet aggregation and rapid emulsion separation.

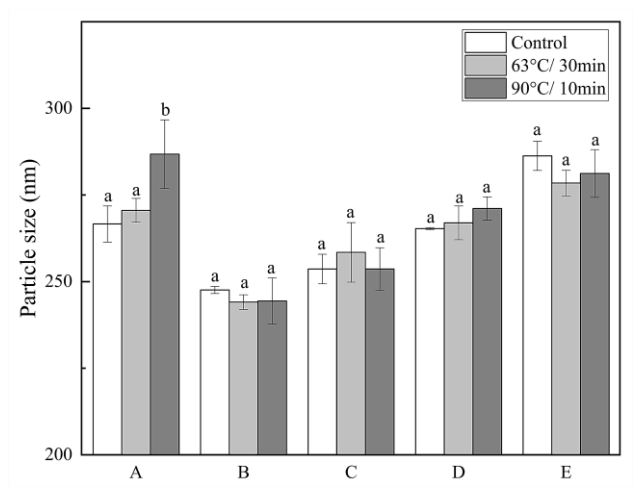


**Figure 9.** Effect of heat-treatment on particle size of emulsion. A, B, C, D, and E represent emulsion samples prepared with five different emulsifiers composed of mixtures of HPI and GS at ratios of 1:0, 0.75:0.25, 0.5:0.5, 0.25:0.75, and 0:1, respectively. Different lowercase letters on error bars indicate significant difference among emulsifier groups by Fisher's LSD test (p < 0.05).

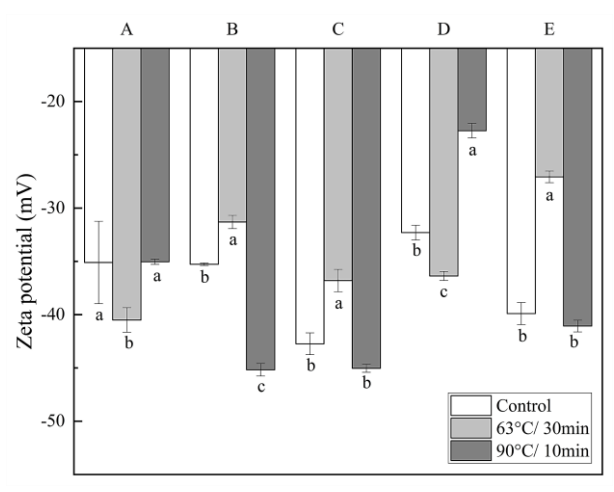


**Figure 10.** Effect of heat-treatment on zeta potential of emulsion. A, B, C, D, and E represent emulsion samples prepared with five different emulsifiers composed of mixtures of HPI and GS at ratios of 1:0, 0.75:0.25, 0.5:0.5, 0.25:0.75, and 0:1, respectively. Different lowercase letters on error bars indicate significant difference among emulsifier groups by Fisher's LSD test (p < 0.05).

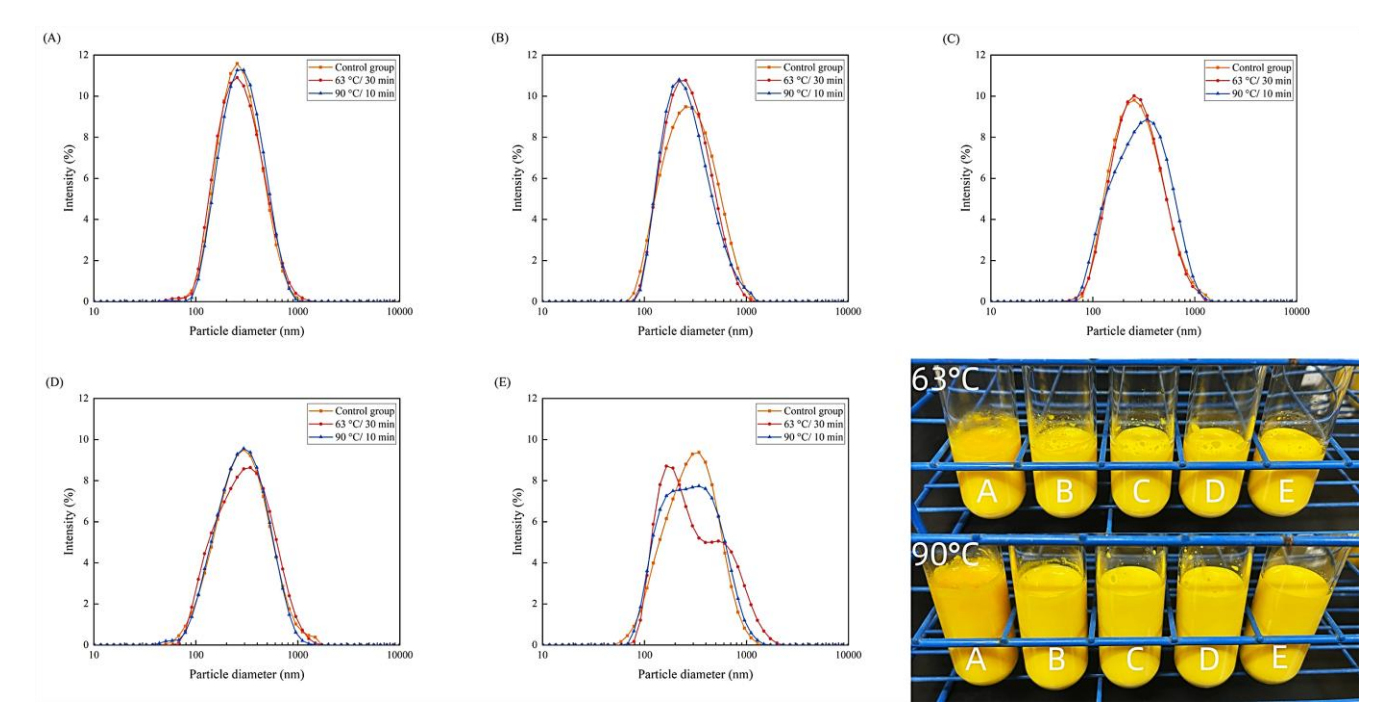
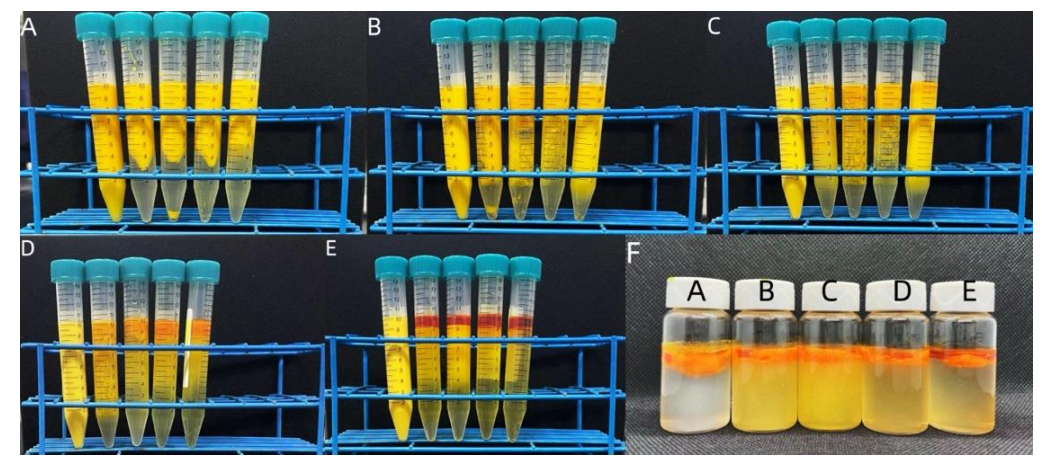


Figure 11. Effect of heat-treatment on particle size distribution and visual images.



**Figure 12.** Effect of ionic strength and freeze-thaw on emulsion. Figures A, B, C, D, and E showed images of emulsions A, B, C, D, and E, respectively, following addition of different amounts of sodium chloride and placement at room temperature for 12 h. From left to right, amounts added were 0, 50, 100, 250, and 500 mM.

Additionally, the freeze-thaw cycle results of the five emulsions showed that any emulsion will experience complete oil-water separation after just one freeze-thaw cycle. This occurred because, after freezing, the droplets in the emulsion became more tightly packed due to the reduced volume of water molecules. The increased capillary pressure between emulsion droplets led to emulsion breakdown, causing oil droplet coalescence and stratification during thawing (Salminen et al., 2020). Currently, there is minimal research on enhancing the freezethaw stability of emulsions containing HPI. According to previous reports, appropriate protein hydrolysis and conjugation with polysaccharides may improve freeze-thaw stability (Mun et al., 2008; Zhang et al., 2019). The utilisation of cryoprotectants in emulsion may relieve the separation of emulsion. Furthermore, emulsion stability can be improved by selecting appropriate components, such as the type of oil, emulsifier, and biopolymers, or by controlling parameters during the freezing and thawing processes (Degner et al., 2014).

In summary, this emulsion exhibited poor stability against ionic strength and freeze-thaw cycles, suggesting that such conditions should be avoided in subsequent product applications.

# Conclusion

The present work elucidated the potential of HPI and GS mixtures as effective emulsifiers for stable emulsion formulations. Emulsions prepared with mixed HPI-GS emulsifiers exhibited smaller particle sizes, higher zeta potentials and encapsulation efficiency, and more uniform particle size distribution, all of which are critical for maintaining stability. However, emulsions exhibited poor stability under ionic strength and freeze-thaw conditions, suggesting limitations in certain applications. Future studies will investigate the in vitro simulated digestion of emulsions, and examine their effectiveness in enhancing the bioavailability of functional lipids. Additionally, the distinctive aroma of palm functional lipids and bitterness imparted by ginsenosides may have unexpected roles in future food applications. Overall, the findings highlighted that specific ratios of HPI-GS mixtures could significantly enhance emulsion stability, offering valuable insights for the development of robust emulsion-based products.

#### Acknowledgement

The first author received financial support from the China Scholarship Council (CSC). The present work was also financially supported by the Ministry of Higher Education, Malaysia through the Fundamental Research Grant Scheme (grant no.: FRGS/1/2020/WAB04/UPM/01/4).

#### References

Chae, S., Kang, K. A., Youn, U., Park, J. S. and Hyun, J. W. 2010. A comparative study of the potential antioxidant activities of ginsenosides. Journal of Food Biochemistry 34: 31-43.

Chen, J., He, J., Zhao, Z., Li, X., Tang, J., Liu, Q. and Wang, H. 2023. Effect of heat treatment on the

- physical stability, interfacial composition and protein-lipid co-oxidation of whey protein isolate-stabilised O/W emulsions. Food Research International 172: 113126.
- Chen, J., Li, F., Li, Z., McClements, D. J. and Xiao, H. 2017. Encapsulation of carotenoids in emulsion-based delivery systems: Enhancement of β-carotene water-dispersibility and chemical stability. Food Hydrocolloids 69: 49-55.
- Chen, X.-W., Wang, T.-G., Yin, W.-J., Zhang, L.-S. and Sun, S.-D. 2024. All-natural plant-based HIPE-gels simultaneously stabilizing with Quillaja saponin and soy protein isolate: Influence of environmental stresses on stability. Food Hydrocolloids 151: 109880.
- Colombo, M. L. 2010. An update on vitamin E, tocopherol and tocotrienol—perspectives. Molecules 15(4): 2103-2113.
- Degner, B. M., Chung, C., Schlegel, V., Hutkins, R. and McClements, D. J. 2014. Factors influencing the freeze-thaw stability of emulsion-based foods. Comprehensive Reviews in Food Science and Food Safety 13(2): 98-113.
- Evans, M., Ratcliffe, I. and Williams, P. A. 2013. Emulsion stabilisation using polysaccharide-protein complexes. Current Opinion in Colloid and Interface Science 18(4): 272-282.
- Feng, Y., Yuan, D., Cao, C., Kong, B., Sun, F., Xia, X. and Liu, Q. 2022. Changes of *in vitro* digestion rate and antioxidant activity of digestion products of ethanol-modified whey protein isolates. Food Hydrocolloids 131: 107756.
- Fu, J.-Y., Che, H.-L., Tan, D. M.-Y. and Teng, K.-T. 2014. Bioavailability of tocotrienols: Evidence in human studies. Nutrition and Metabolism 11: 1-10.
- Gallagher, W. 2009. FTIR analysis of protein structure. United States: University of Wisconsin-Eau Claire.
- Gholivand, S., Tan, T. B., Yusoff, M. M., Choy, H. W., Teow, S. J., Wang, Y., ... and Tan, C. P. 2024. Elucidation of synergistic interactions between anionic polysaccharides and hemp seed protein isolate and their functionalities in stabilizing the hemp seed oil-based nanoemulsion. Food Hydrocolloids 146: 109181.

- Goh, P. S., Ng, M. H., Choo, Y. M., Nasrulhaq Boyce, A., and Chuah, C. H. 2015. Production of nanoemulsions from palm-based tocotrienol rich fraction by microfluidization. Molecules 20(11): 19936-19946.
- Han, C., Ren, X., Shen, X., Yang, X. and Li, L. 2024. Improvement of physicochemical properties and quercetin delivery ability of fermentation-induced soy protein isolate emulsion gel processed by ultrasound. Ultrasonics Sonochemistry 107: 106902.
- Igartúa, D. E., Dichano, M. C., Ferrari, S. B., Palazolo, G. G. and Cabezas, D. M. 2024. Combination of pH-shifting, ultrasound, and heat treatments to enhance solubility and emulsifying stability of rice protein isolate. Food Chemistry 433: 137319.
- Jourdain, L. S., Schmitt, C., Leser, M. E., Murray, B. S. and Dickinson, E. 2009. Mixed layers of sodium caseinate + dextran sulfate: Influence of order of addition to oil-water interface. Langmuir 25(17): 10026-10037.
- Karabulut, G., Feng, H. and Yemiş, O. 2022. Physicochemical and antioxidant properties of industrial hemp seed protein isolate treated by high-intensity ultrasound. Plant Foods for Human Nutrition 77(4): 577-583.
- Kaspchak, E., Kayukawa, C. T. M., Silveira, J. L. M., Igarashi-Mafra, L. and Mafra, M. R. 2020. Interaction of Quillaja bark saponin and bovine serum albumin: Effect on secondary and tertiary structure, gelation and *in vitro* digestibility of the protein. LWT Food Science and Technology 121: 108970.
- Kim, W., Wang, Y. and Selomulya, C. 2020. Dairy and plant proteins as natural food emulsifiers. Trends in Food Science and Technology 105: 261-272.
- Li, H., Cai, Y., Li, F., Zhang, B., Wu, X. and Wu, W. 2022. Rancidity-induced protein oxidation affects the interfacial dynamic properties and the emulsion rheological behavior of rice bran protein. Food Hydrocolloids 131: 107794.
- Li, J., Li, F. and Jin, D. 2023a. Ginsenosides are promising medicine for tumor and inflammation: A review. The American Journal of Chinese Medicine 51(04): 883-908.
- Li, M., Ritzoulis, C., Du, Q., Liu, Y., Ding, Y., Liu, W. and Liu, J. 2021. Recent progress on protein-polyphenol complexes: Effect on

- stability and nutrients delivery of oil-in-water emulsion system. Frontiers in Nutrition 8: 765589.
- Li, Y., Liu, X., Liu, H. and Zhu, L. 2023b. Interfacial adsorption behavior and interaction mechanism in saponin-protein composite systems: A review. Food Hydrocolloids 136: 108295.
- Lima, R. R., Stephani, R., Perrone, Í. T. and de Carvalho, A. F. 2023. Plant-based proteins: A review of factors modifying the protein structure and affecting emulsifying properties. Food Chemistry Advances 3: 100397.
- Liu, H., Zhu, X., Jiang, Y., Sun-Waterhouse, D., Huang, Q., Li, F. and Li, D. 2021. Physicochemical and emulsifying properties of whey protein isolate (WPI)-polydextrose conjugates prepared *via* Maillard reaction. International Journal of Food Science and Technology 56(8): 3784-3794.
- Liu, X., Xue, F. and Adhikari, B. 2023a. Hemp protein isolate-polysaccharide complex coacervates and their application as emulsifiers in oil-in-water emulsions. Food Hydrocolloids 137: 108352.
- Liu, X., Xue, F. and Adhikari, B. 2023b. Production of hemp protein isolate-polyphenol conjugates through ultrasound and alkali treatment methods and their characterization. Future Foods 7: 100210.
- Lowry, G. V., Hill, R. J., Harper, S., Rawle, A. F., Hendren, C. O., Klaessig, F., ... and Rumble, J. 2016. Guidance to improve the scientific value of zeta-potential measurements in nanoEHS. Environmental Science Nano 3(5): 953-965.
- Ma, W., Wang, J., Wu, D., Xu, X., Wu, C. and Du, M. 2020. Physicochemical properties and oil/water interfacial adsorption behavior of cod proteins as affected by high-pressure homogenization. Food Hydrocolloids 100: 105429.
- Mba, O. I., Dumont, M.-J. and Ngadi, M. 2015. Palm oil: Processing, characterization and utilization in the food industry—A review. Food Bioscience 10: 26-41.
- McClements, D. J. and Decker, E. 2018. Interfacial antioxidants: A review of natural and synthetic emulsifiers and coemulsifiers that can inhibit lipid oxidation. Journal of Agricultural and Food Chemistry 66(1): 20-35.

- Mun, S., Cho, Y., Decker, E. A. and McClements, D. J. 2008. Utilization of polysaccharide coatings to improve freeze—thaw and freeze—dry stability of protein-coated lipid droplets. Journal of Food Engineering, 86(4): 508-518.
- Rajasekaran, B., Singh, A., Ponnusamy, A., Patil, U., Zhang, B., Hong, H. and Benjakul, S. 2023. Ultrasound treated fish myofibrillar protein: Physicochemical properties and its stabilizing effect on shrimp oil-in-water emulsion. Ultrasonics Sonochemistry 98: 106513.
- Salminen, H., Bischoff, S. and Weiss, J. 2020. Formation and stability of emulsions stabilized by Quillaja saponin-egg lecithin mixtures. Journal of Food Science 85(4): 1213-1222.
- Salvia-Trujillo, L., Qian, C., Martín-Belloso, O. and McClements, D. J. 2013. Influence of particle size on lipid digestion and β-carotene bioaccessibility in emulsions and nanoemulsions. Food Chemistry 141(2): 1472-1480.
- Sharif, H. R., Sharif, M. K. and Zhong Fang, Z. F. 2017. Preparation, characterization and rheological properties of vitamin E enriched nanoemulsion. Pakistan Journal of Food Sciences 27(1): 7-14.
- Shen, P., Gao, Z., Fang, B., Rao, J. and Chen, B. 2021. Ferreting out the secrets of industrial hemp protein as emerging functional food ingredients. Trends in Food Science and Technology 112: 1-15.
- Shi, L. S., Yang, X. Y., Gong, T., Hu, C. Y., Shen, Y. H. and Meng, Y. H. 2023. Ultrasonic treatment improves physical and oxidative stabilities of walnut protein isolate-based emulsion by changing protein structure. LWT Food Science and Technology 173: 114269.
- Shishir, M. R. I., Xie, L., Sun, C., Zheng, X. and Chen, W. 2018. Advances in micro and nanoencapsulation of bioactive compounds using biopolymer and lipid-based transporters. Trends in Food Science and Technology 78: 34-60.
- Silva, J. V., Jacquette, B., Amagliani, L., Schmitt, C., Nicolai, T. and Chassenieux, C. 2019. Heat-induced gelation of micellar casein/plant protein oil-in-water emulsions. Colloids and Surfaces A Physicochemical and Engineering Aspects 569: 85-92.
- Sun, S., Zhang, C., Li, S., Yan, H., Zou, H. and Yu, C. 2023. Improving emulsifying properties

- using mixed natural emulsifiers: Tea saponin and golden pompano protein. Colloids and Surfaces A Physicochemical and Engineering Aspects 656: 130311.
- Sundram, K., Sambanthamurthi, R. and Tan, Y.-A. 2003. Palm fruit chemistry and nutrition. Asia Pacific Journal of Clinical Nutrition 12(3): 355-362.
- Tan, P. Y., Tey, B. T., Chan, E. S., Lai, O. M., Chang,
  H. W., Tan, T. B., ... and Tan, C. P. 2021.
  Stabilization and release of palm tocotrienol emulsion fabricated using pH-sensitive calcium carbonate. Foods 10(2): 358.
- Tian, T., Ko, C.-N., Li, D. and Yang, C. 2023. The anti-aging mechanism of ginsenosides with medicine and food homology. Food and Function 14: 9123-9136.
- Wang, Z., Li Y., Jiang, L., Qi, B. and Zhou, L. 2014. Relationship between secondary structure and surface hydrophobicity of soybean protein isolate subjected to heat treatment. Journal of Chemistry 2024: 475389.
- Wilde, P., Mackie, A., Husband, F., Gunning, P. and Morris, V. 2004. Proteins and emulsifiers at liquid interfaces. Advances in Colloid and Interface Science 108: 63-71.
- Wu, T., Lin, L., Zhang, X., Wang, X. and Ding, J. 2023. Covalent modification of soy protein hydrolysates by EGCG: Improves the emulsifying and antioxidant properties. Food Research International 164: 112317.
- Xiao, X., Zou, P.-R., Hu, F., Zhu, W. and Wei, Z.-J. 2023. Updates on plant-based protein products as an alternative to animal protein: Technology, properties, and their health benefits. Molecules 28(10): 4016.
- Xu, L., Zhang, M., Hong, X., Liu, Y. and Li, J. 2021. Application of ultrasound in stabilizing of Antarctic krill oil by modified chickpea protein isolate and ginseng saponin. LWT - Food Science and Technology 149: 111803.
- Xu, Y., Sismour, E., Britland, J. W., Sellers, A., Abraha-Eyob, Z., Yousuf, A., ... and Zhao, W. 2022. Physicochemical, structural, and functional properties of hemp protein vs several commercially available plant and animal proteins: A comparative study. ACS Food Science and Technology 2(10): 1672-1680.
- Xue, F., Li, C. and Adhikari, B. 2020. Physicochemical properties of soy protein

- isolates-cyanidin-3-galactoside conjugates produced using free radicals induced by ultrasound. Ultrasonics Sonochemistry 64: 104990.
- Yan, S., Xu, J., Liu, G., Du, X., Hu, M., Zhang, S., ... and Li, Y. 2022. Emulsions co-stabilized by soy protein nanoparticles and tea saponin: Physical stability, rheological properties, oxidative stability, and lipid digestion. Food Chemistry 387: 132891.
- Zhang, A., Yu, J., Wang, G., Wang, X., and Zhang, L. 2019. Improving the emulsion freeze-thaw stability of soy protein hydrolysate-dextran conjugates. LWT - Food Science and Technology 116: 108506.
- Zhang, R., Chen, H., Wu, Y., Yu, Y., Yuan, J., Lv, C. and Lu, J. 2024. Changes in the physicochemical characteristics and biological activities of polysaccharides from Panax ginseng during defense against red-skin disease. Industrial Crops and Products 208: 117865.
- Zhang, X., Wang, Q., Liu, Z., Zhi, L., Jiao, B., Hu, H., ... and Shi, A. 2023. Plant protein-based emulsifiers: Mechanisms, techniques for emulsification enhancement and applications. Food Hydrocolloids, 109008.